Paper ID APEN-MIT-2020_330
Applied Energy Symposium: MIT A+B
August 12-14, 2020 • Cambridge, USA

Model-based control of alkaline pretreatment for enhanced cellulose accessible surface area

Hyun-Kyu Choi
Artie McFerrin Department of Chemical Engineering
Texas A&M University
Texas A&M Energy Institute
College Station, TX, United States
nicechoi@tamu.edu

Joseph Sang-Il Kwon
Artie McFerrin Department of Chemical Engineering
Texas A&M University
Texas A&M Energy Institute
College Station, TX, United States
kwonx075@tamu.edu

***Abstract*— It is widely recognized that cellulose accessibility is closely connected to sugar yield which determines economic viability of biorefining. However, existing kinetic models are not able to capture the evolution of the microscopic properties of biomass (e.g., cellulose accessibility) during pretreatment. Motivated by the limitation, we developed a multiscale model that is capable of describing the dynamic evolution of cellulose accessible area by integrating a macroscopic kinetic model with a microscopic kinetic Monte Carlo model. Then, a model reduction technique is employed to lower the computational complexity of the multiscale model, and employed to a model-based feedback controller to enhance the cellulose accessibility while minimizing the heat during alkaline pretreatment. The implementation of the control framework improved the glucose yield by 19.9% compared to a conventional constant-temperature pretreatment method.**

Keywords—cellulose accessibility, accessible surface area, multiscale model, model-based control, alkaline pretreatment

I. INTRODUCTION

As a sustainable substitute for petroleum-derived fuel, biofuels have attracted much attention over the last few decades [1, 2]. In more recent days, since fuel-conversion of agricultural crops, whose supply can be limited due to the competition with the food industry, the use of lignocellulosic biomass (i.e., woody biomass) comes under the extensive spotlight [3, 4]. However, since the conversion of lignocellulosic biomass is relatively expensive hurting the economic viability of cellulosic biofuel production, optimization of the process operation is a key to the success of the biorefining industry. Among the biorefining stages, formation of fermentable glucose (i.e., a simple sugar that constructs cellulose) has become a bottle-neck for commercialization of cellulosic biofuel production due to compact and rigid structure of lignocellulosic biomass known as recalcitrance [1, 5].

Since the inherent recalcitrance of lignocellulosic biomass helps resisting its degradation into structural carbohydrates by enzymes, some preprocesses (i.e., pretreatment, mechanical refining) are typically applied before the cellulose hydrolysis to open up biomass structure and make cellulose more accessible to enzymes [6]. It has been widely recognized that a pretreatment step is very important to disrupt the recalcitrant structure by removing a lignin barrier (i.e., delignification) and increase the cellulose accessible surface area (ASA) for improved biomass enzymatic digestibility [1, 7]; because a high sugar yield can be achieved when enzymes can easily access to the surface of cellulose [5].

During the last decade, a number of pretreatment techniques have been developed for bioconversion of lignocellulosic biomass. Although the mechanisms of these pretreatment methods are different, the objective is to enhance cellulose ASA for efficient hydrolysis by either chemical or enzymes. Among the pretreatment methods, alkaline pretreatment, which is a chemical pretreatment type, has received more attention as it is relatively cost effective and energy efficient than other methods [8, 9]. Sodium hydroxide (NaOH) is one of the most effective alkaline reagents, and has been utilized for pretreatment of diverse lignocellulosic biomass mostly at elevated temperature [10]. Nevertheless, due to the lack of knowledge on the evolution of microconfiguration of biomass during pretreatment, a control framework that can possibly predict cellulose ASA and energy consumption has not been designed.

While there are some kinetic models for pretreatment in the literature, they are not able to capture the evolution of microscopic biomass properties such as ASA [11, 12]. Motivated by this limitation, we propose a multiscale model of alkaline pretreatment to describe the evolution of cellulose ASA during the pretreatment process. Then, utilizing this model, we develop a model-based feedback control scheme to simultaneously improve cellulose ASA and minimize the heat usage.

The paper is organized as follows: A multiscale model is presented to describe the evolution of cellulose ASA during alkaline pretreatment by integrating macroscopic and microscopic models. Then, experimental data in the literature is employed to predict the glucose yield from the simulated ASA values. Lastly, a model predictive control (MPC) algorithm for the pretreatment process is developed to enhance cellulose ASA and reduce the heat consumption.

II. MULTISCALE MODELING OF ASA

In this work, a multiscale model of ASA is designed by adopting multiscale models that describe pulp digester [13, 14]. The first principles that are identical to Kraft pulping reaction kinetics are considered to describe the alkaline

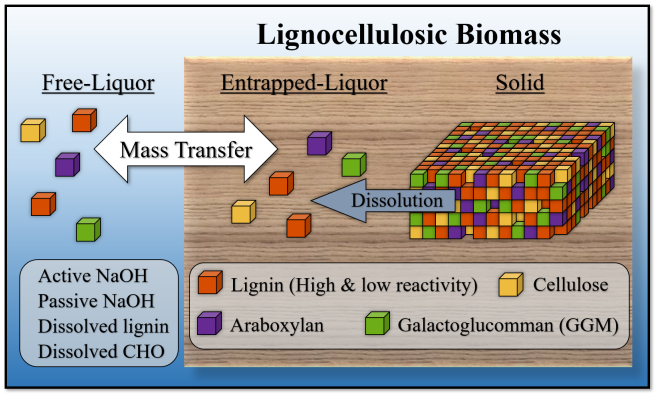

Fig. 1: A pretreatment system composed of three phases with four liquor and five solid components.

(NaOH) pretreatment of lignocellulosic biomass; both processes utilize NaOH to delignify lignocellulosic biomass at high temperature either to make cellulose more accessible or to obtain pure cellulose fibers for papermaking. Accordingly, the system of lignocellulosic biomass in a pretreatment reactor can be described by a widely used Kraft pulping kinetic model (i.e., *Purdue model*). Specifically, Fig. 1 shows the system that consists of solid, entrapped-liquor and free liquor phases. The solid phase describes the dry portion of biomass, the entrapped-liquor phase represents the liquor residing in the pores of biomass, and the free-liquor phase denotes a bulk phase fluid encompassing the solid and entrapped-liquor phases. By integrating the kinetic model with a microscopic model (i.e., kinetic Monte Carlo (kMC) algorithm), a multiscale model that is capable of capturing an ASA evolution within the pretreatment process is developed.

A. Process description

In general, biorefining goes through several processes. After collection of appropriate biomasses, they are pretreated with chemical solvents to increase cellulose accessibility, followed by mechanical refining which further physically deconstruct the biomass structure. Then, enzymes (e.g., cellulase) hydrolyze the cellulose into its monosaccharide unit which is mainly glucose (i.e., a simple sugar). Fermentation converts the sugar to alcohol or acid, which is then separated by distillation for fuel purity. Utilizing these processes, a variety of operation scenarios are possible. For example, intensive refining is required or high enzyme dosage is necessary to meet a target glucose yield when the cellulose ASA from pretreatment process is not satisfactory. Since achieving a relatively high ASA during pretreatment would save the cost associated with subsequent processes such as mechanical refining or enzymatic hydrolysis, pretreatment plays an important role in producing low cost sugars from biomass.

In general, due to its high recalcitrance, lignocellulosic biomass (i.e., wood chips) is cooked intensively in an alkaline pretreatment reactor, where lignin is removed and chemical composition changes to increase cellulose ASA; this process is required as microfibrils are embedded in a matrix of cross-linked lignin that blocks the cellulose surface. By manipulating the operating temperature, we can adjust the extent of the delignification reaction between woody biomass and sodium hydroxide (i.e., through the Arrhenius law) [15, 16]. Typically, alkaline pretreatment is performed at high temperature (70 – 150 C°) for 10 –60 minutes under 2.0% NaOH concentration [6]. During the alkaline pretreatment process, a significant amount of heat is required to elevate and maintain the high temperature, typically consuming 23% of the total operation cost [17].

B. Macroscopic model formulation

The degradation kinetics of biomass during the NaOH pretreatment is described by a simplified version of a Kraft pulping model (i.e., extended Purdue model) [16, 18]. In this work, five solid components are considered for the solid phase: high reactivity lignin(s_1), low reactivity lignin (s_2), cellulose (s_3), araboxylan (s_4) and galactoglucomman (GGM) (s_5). Although six liquor components are considered in the original Purdue model, due to the absence of sulfuric acid in alkaline pretreatment, only four liquor components are considered for the two liquor phases: active NaOH (e_1, f_1), passive NaOH (e_2, f_2), dissolved lignin (e_3, f_3), and dissolved carbohydrates (CHO) (e_4, f_4) (Fig. 1). In the macroscopic modeling framework, the subscripts $i = 1, \ldots, 5$ and $j = 1, \ldots, 4$ denote the solid and the liquor components, respectively.

1) Mass and energy balance equations: Since the reactor is a batch type, the mass balances of the solid phase are equal to their reaction rates as follows:

$$\frac{d\rho_{s_i}}{dt} = R_{s_i} \tag{1}$$

where R_{s_i} is the reaction rate of the solid component i. Then, the mass balance of the entrapped- and free-liquor phases are defined as follows:

$$\frac{d\rho_{e_j}}{dt} = R_{e_j} + D\left(\rho_{f_j} - \rho_{e_j}\right) \tag{2a}$$

$$\frac{d\rho_{f_j}}{dt} = D\epsilon\frac{(1-\eta)}{\eta}\left(\rho_{e_j} - \rho_{f_j}\right) \tag{2b}$$

where R_{e_j} is the reaction rate of the entrapped-liquor component j, D is the average mass diffusivity of the four liquor components to consider the mass transport between two liquor phases, ϵ is the biomass porosity, and η is the biomass compaction factor which takes into account the swelling of biomass during pretreatment. Note that the mass balance of the free-liquor phase does not include the reaction rate term since the solid degradation reaction is assumed to take place only at the surface of the solid and entrapped-liquor phases.

Assuming that the heat transfer coefficient between the solid and entrapped-liquor phases is very large, a single temperature value is considered for the two phases which is defined as T_c, namely a chip phase temperature. Therefore, the temperatures of chip phase (T_c) and free-liquor phase (T_f) are considered for the given pretreatment system. On

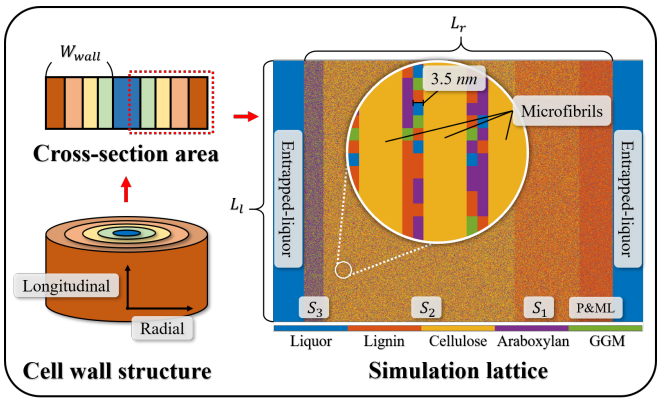

Fig. 2: Schematic illustration of the simulation lattice.

the basis of the above assumption, the energy balance of the chip phase is defined as below:

$$\left(C_{p_s} M_s + C_{p_e} M_e \epsilon\right) \frac{dT_c}{dt} = U\left(T_f - T_c\right) + D\epsilon D_E + \Delta H_R \sum_{i=1}^{5} R_{s_i} \tag{3}$$

where C_{p_s} and C_{p_e} are the heat capacities of the solid and entrapped-liquor phases, respectively, M_s and M_e are the total masses of the two phases, respectively, U is the heat transfer coefficient between the two liquor phases, D_E is the amount of energy transported to the entrapped-liquor from the free-liquor phase by diffusion, and ΔH_R is the heat of reaction.

Then, the energy balance of free-liquor phase is given as:

$$\left(Cp_f M_f\right) \frac{dT_f}{dt} = U\left(T_c - T_f\right) - D\epsilon \frac{(1-\eta)}{\eta} D_E \tag{4}$$

where Cp_f and M_f are the heat capacity and total mass of the free-liquor phase.

The detailed model derivation and parameter values are documented in references [13, 14]

C. Microscopic model formulation

The conventional macroscopic models are not able to capture the evolution of biomass microscopic properties such as cellulose accessibility. Motivated by this consideration, a microscopic model (i.e., kMC algorithm) is hybridized with the macroscopic model to describe the evolution of cellulose ASA during alkaline pretreatment. Modeling of the cellulose ASA via kMC simulation is explained in this section.

1) Simulation lattice formation: In order to capture the microscopic properties, a 2-dimensional axisymmetric simulation lattice is introduced and used for simulating the spatially-resolved biomass microconfiguration (Figs. 2 and 3). The initial configuration of the five solid components is considered in each layer based on their chemical composition; lignocellulose typically has a hierarchical structure which consists of primary wall and middle lamella (P & ML), and secondary wall layers (S_1, S_2 and S_3) [19]. The number of radial and longitudinal lattice sites are denoted by L_r and L_l, respectively, and periodic boundary conditions are applied on both the longitudinal directions (Fig. 2). The length of a single square-shaped lattice site is set to be 3.5 nm which is the diameter of dissolved lignin and cellulose elementary fibril [20].

In this work, Norway Spruce is selected as lignocellulose feedstock whose properties such as chemical composition of each layer and cell wall thickness (W_{wall}) are employed to initialize the simulation lattice sites; Norway spruce (Picea abies) is one of the most commonly used materials for Northern Bleached Softwood Kraft (NBSK) pulp whose production volume is rated as the second largest in the world by tonnage.

2) Implementation of kMC algorithm: A kMC algorithm is applied to describe the evolution of biomass microconfiguration by utilizing the balance equations (1)–(4), and the initialized simulation lattice. The total solid degradation reaction rate is defined as follows:

$$R_{tot} = \sum_{i=1}^{5} R_{s_i} \tag{5}$$

Then, the ratios of the individual rates to the total rate are computed to infer the probability of each degradation event as presented in Table I, followed by drawing a random number, $\xi_1 \in (0, 1]$, to select the solid component which will be removed from the simulation lattice sites. After the selection, another random number, i.e., $\xi_2 \in (0, N_{s_i}]$, is generated to determine which site of the selected solid component will dissolve, where N_{s_i} denotes the number of unreacted s_i sites on the lattice.

Then, the concentration and temperature of the entrapped-liquor and free-liquor phases are updated by (1)–(4). Lastly, the elapsed time of the executed event is computed as follows:

$$\Delta t = \frac{-\ln \xi_3}{R_{tot}} \tag{6}$$

where $\xi_3 \in (0, 1]$ is an additionally drawn random number.

The series of operations will be repeated until the accumulated event time reaches the user-defined final time (t_{final}); typically, alkaline pretreatment operates for 10–60 minutes [6].

3) Cellulose ASA calculation: During the pretreatment process, lignin barrier dissolves faster than cellulose due to the stability difference under the alkaline condition. As a

TABLE I: The probability conditions and corresponding events.

Probability Conditions	**Executed Event**
$0 < \xi_1 \leq \frac{R_{s_1}}{R_{tot}}$	Degradation of s_1
$\frac{R_{s_1}}{R_{tot}} < \xi_1 \leq \frac{R_{s_1}+R_{s_2}}{R_{tot}}$	Degradation of s_2
$\frac{R_{s_1}+R_{s_2}}{R_{tot}} < \xi_1 \leq \frac{R_{s_1}+R_{s_2}+R_{s_3}}{R_{tot}}$	Degradation of s_3
$\frac{R_{s_1}+R_{s_2}+R_{s_3}}{R_{tot}} < \xi_1 \leq \frac{R_{s_1}+R_{s_2}+R_{s_3}+R_{s_4}}{R_{tot}}$	Degradation of s_4
$\frac{R_{s_1}+R_{s_2}+R_{s_3}+R_{s_4}}{R_{tot}} < \xi_1 \leq 1$	Degradation of s_5

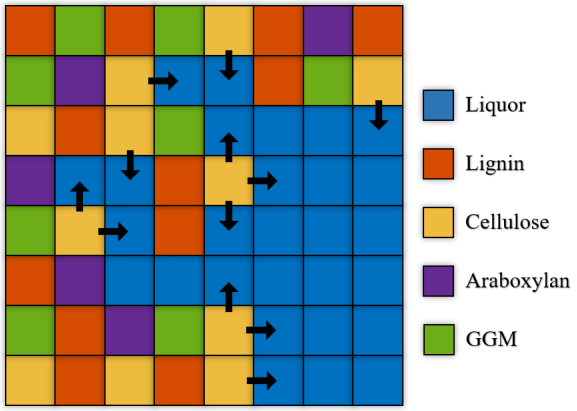

Fig. 3: Schematic illustration of the calculation of cellulose ASA.

result, the surface of cellulose gets uncovered and accessible for enzymatic hydrolysis. The evolution of the cellulose ASA is taken into account by counting the number of open sites which are in contact with the entrapped-liquor phase as follows:

$$A_c = \frac{N_{o,s_3}}{N_{o,s_1} + N_{o,s_2} + N_{o,s_3} + N_{o,s_4} + N_{o,s_5}} \tag{7}$$

where A_c is the ASA of cellulose, and N_{o,s_i} is the total number of component sites of s_i that are in contact with the entrapped-liquor. For example, the number of black arrows in Fig. 3 represents that of cellulose, N_{o,s_3}.

D. Prediction of glucose yield

In order to predict the glucose yield from the proposed ASA modeling, experimentally measured glucose yield data in reference [21] is used to fit the kMC simulation results as follow:

$$Y_g = \alpha \cdot A_c \tag{8}$$

where α is a scalar parameter that connects the simulated ASA and glucose yield (Y_g)); please note that α has been obtained by utilizing multiple sets of experimental data. The idea behind introducing this experimentally verified α is that glucose yield by enzymatic hydrolysis is directly determined by cellulose ASA [22].

Specifically, the yields under two different operating conditions are used to determine the scalar parameter, α; the two conditions are presented in Table. II where the sample 1 is for untreated biomass. The scalar parameter is computed by minimizing the errors between the predicted values and the experiment data as follows:

$$\min_{\alpha} \left(\alpha \cdot A_{c,1} - Y_{g,1}\right)^2 + \left(\alpha \cdot A_{c,2} - Y_{g,2}\right)^2 \tag{9}$$

where $A_{c,i}$ and $Y_{g,i}$ are the simulated ASA and glucose yield values from the i^{th} sample, respectively.

TABLE II: The operating conditions of the pretreated samples.

Conditions and yield	**Sample 1**	**Sample 2**
Temperature (T_f)	N/A	120 C°
Residence time (t_{final})	N/A	60 min
NaOH concentration (ρ_{f_1})	N/A	2.0%
Glucose yield (48h)	14.7%	56.2%

III. Model-based feedback controller design

In this section, a model-based feedback controller is designed for alkaline pretreatment. The objective of the controller is to enhance cellulose ASA while mitigating the pretreatment heat usage by manipulating the free-liquor phase temperature (i.e., bulk phase temperature). A discrete-time linear model is identified, which will be used to design a state estimator. The implementation of a model predictive control (MPC) strategy is described in this section.

A. Model reduction method and state estimator

As the employed macroscopic model (i.e., *extended Purdue model*) consists of 19 nonlinear ordinary equations, a reduced-order model is required to mitigate the computational complexity. Specifically, multivariable output error state space (MOESP) algorithm is used to identify a state-space model that is in the following linear discrete time-invariant form:

$$x_{t_{k+1}} = Ax_{t_k} + Bu_{t_k} \tag{10a}$$
$$y_{t_k} = Cx_{t_k} + v_{t_k} \tag{10b}$$

where x_{t_k} is the state variables of the reduced-order model, u_{t_k} is the manipulated input variable (i.e., T_f), y_{t_k} is the output variable (i.e, Y_g), and v_{t_k} is an unknown noise which is considered to be zero mean Gaussian white [23].

Then, a Kalman filter (i.e., state estimator) is designed to estimate the states from the measurement at every sampling time ($t = t_k$). The Kalman filter gain (M_{t_k}), which is determined at every time steps, leads to a correction of the state estimates ($\hat{x}_{t_k}$) and the error covariance (P_{t_k}) as follows:

$$M_{t_k} = P_{t_k|t_{k-1}} C^T \left(R_{t_k} + C P_{t_k|t_{k-1}} C^T\right)^{-1} \tag{11a}$$
$$\hat{x}_{t_k} = A\hat{x}_{t_k|t_{k-1}} + Bu_{t_k} + M_{t_k}\left(y_{t_k} - \hat{y}_{t_k|t_{k-1}}\right) \tag{11b}$$
$$P_{t_k} = \left(I - M_{t_k} C\right) P_{t_k|t_{k-1}} \tag{11c}$$

where I denotes the identity matrix. The estimated state variables in (11b) are used to predict the future state and output variables through (10).

B. Model predictive control (MPC) formulation

A MPC scheme is applied to the alkaline pretreatment process by using the developed Kalman filter that predicts the future behavior of the system. The controller is designed to compute an input sequence in which a defined cost function is optimized subject to the given constraints in the following form:

$$\min_{T_{f_k},\ldots,T_{f_{N_p}}} \sum_{i=k}^{N_p-1} \omega_1 \left(T_{f_i}\right)^2 + \omega_2 \left(Y_{g,t_{N_p}} - Y_{g,set}\right)^2 \quad (12a)$$

$$\text{s.t.} \quad \text{Kalman filter}, \ (10)-(11) \quad (12b)$$

$$T_{f_{min}} \leq T_{f_{k+m}} \leq T_{f_{max}} \quad (12c)$$

$$\frac{|T_{f_k} - T_{f_{k+1}}|}{\Delta} \leq R_{T_f} \quad (12d)$$

$$m = 1, \ldots, N_p - k$$

where ω_1 and ω_2 denote the weighting parameters for the manipulated input and the endpoint output variable deviation, respectively, $Y_{g,set}$ is a set-point value for the output variable, $T_{f_{min}}$ and $T_{f_{max}}$ are the operating temperature boundaries of the pretreatment reactor which serve as an input constraint, Δ is the sampling interval, T_{f_k} is the free-liquor temperature at k^{th} sampling time which stays constant until the next sampling period, and R_{T_f} is the maximum input change rate to prevent an abrupt temperature jump.

Under the shrinking horizon framework (i.e., $N_p = \frac{t_{final}-t_k}{\Delta}$), the trajectory of the manipulated input $(T_{f_k}, \ldots, T_{f_{N_p}})$ is optimized by solving (12). The cost function (12a) is formulated to simultaneously improve the cellulose ASA and minimize the heat usage for enhanced profitability of pretreatment. The system parameters of the employed MPC are summarized in Table III.

IV. Closed-loop simulation results

MATLAB® R2019a with Intel® Core™ i7-4790 CPU @ 3.60 GHz and 16 GB RAM is utilized for the dynamic kMC simulations and MPC calculations. Conventional alkaline pretreatment has been performed under a constant temperature, while the proposed method manipulated the bulk phase temperature to increase cellulose ASA which in turn improves enzymatic digestibility. In order to demonstrate the advantage of the proposed approach over the conventional method, glucose yield and heat energy consumption from the both methods are compared.

Under the closed-loop operation with the identical initial conditions (e.g., residence time and NaOH concentration), 19.9% higher glucose yield is achieved by consuming only 1.4% more energy compared to the constant temperature operation (i.e., a conventional operating strategy), as described in Table IV. The energy consumption is computed on the basis of the free-liquor temperature during the pretreatment. Even though the same amount of alkaline solvent and residence time are utilized for the pretreatment process, the significant improvement in glucose yield is observed. The significantly enhanced yield would compensate for the slight increase in energy consumption; therefore, the proposed MPC system is more advantageous than the conventional constant temperature pretreatment.

TABLE III: List of MPC system parameters

MPC parameters	**Notations**	**Values**
Number of prediction horizons	N_p	12
Sampling interval	Δ	5 minutes
Weight on the input	ω_1	100
Weight on the output	ω_2	50
Output set-point	$Y_{g,set}$	90
Input Constraints	**Notations**	**Values**
Upper temperature boundary	$T_{f_{max}}$	147 C°
Lower temperature boundary	$T_{f_{min}}$	117 C°
Maximum temperature change rate	R_{T_f}	1 C°/min

TABLE IV: Operating conditions and results of the open-loop and closed-loop operations.

Conditions	**Open-loop**	**Closed-loop**
Residence time (t_{final})	60 min	60 min
NaOH concentration (ρ_{f_1})	2.0%	2.0%
Glucose yield	56.2%	76.1%
Energy consumption	100.0%	101.4%

The closed-loop input and output profiles (i.e., Free-liquor temperature and cellulose ASA) are presented in Figs. 4 and 5, respectively. Relatively intensive heat is applied after 30 minutes of pretreatment whereas the cellulose ASA shows a steady increase along the time, implying that more heat usage than the first half is required to achieve a similar degradation rate due to the low alkaline concentration. While the operation under a constant temperature is not able to handle the negative impact of the decreased NaOH concentration, the closed-loop operation is more effective in dealing with the reduced alkaline reagent.

V. Conclusions

In this work, a multiscale model was developed by integrating a widely used kinetic model with a microscopic model in order to describe the evolution of cellulose ASA

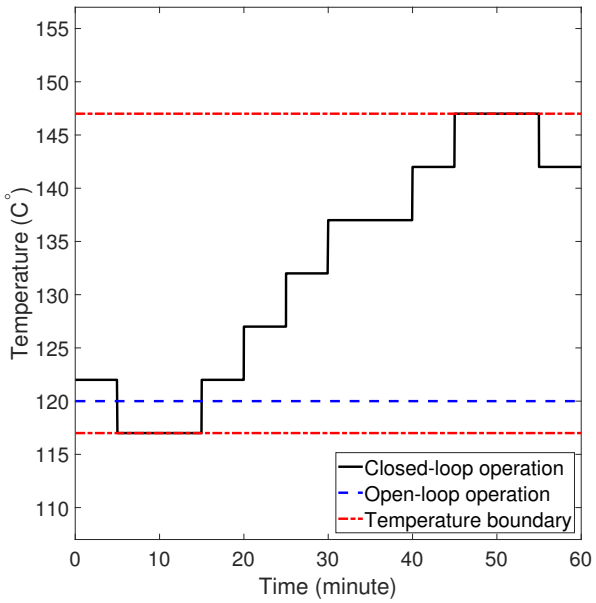

Fig. 4: Free-liquor phase temperature profiles under both closed-loop and open-loop operations.

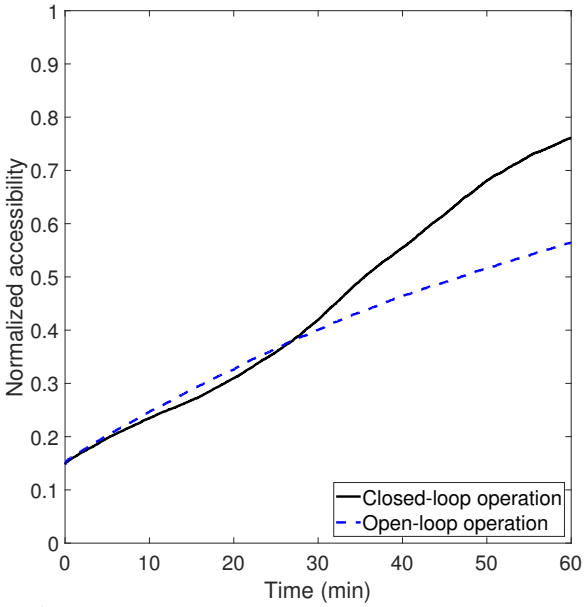

Fig. 5: Normalized cellulose ASA profiles under both closed-loop and open-loop operations.

during pretreatment process. A reduced-order model was identified to reduce the computational complexity of the multiscale model, which is then implemented to a MPC system to improve cellulose ASA while minimizing the heat usage of the pretreatment process. The kMC simulation results demonstrated that the closed-loop operation provides enhanced cellulose ASA under the identical initial conditions.

However, as several microscopic properties of biomass such as lignin concentration, cellulose crystallinity and degree of polymerization can also collectively affect cellulose ASA, incorporation of them into the multiscale model is required to improve the model robustness, which will be a future task. Moreover, recently, mechanical refining techniques are widely used to further destruct the biomass structure to boost cellulose ASA. Therefore, the model coverage can be enlarged by taking into account the effect and energy consumption from the refiner, which is another direction of the future work.

VI. ACKNOWLEDGMENT

Financial support from the Artie McFerrin department of chemical engineering and the Texas A&M Energy Institute are gratefully acknowledged.

REFERENCES

[1] X. Zhao, L. Zhang, and D. Liu, "Biomass recalcitrance. Part II: Fundamentals of different pre-treatments to increase the enzymatic digestibility of lignocellulose," *Biofuels, Bioproducts and Biorefining*, vol. 6, pp. 561–579, 2012.

[2] J. S. Kim, Y. Y. Lee, and T. H. Kim, "A review on alkaline pretreatment technology for bioconversion of lignocellulosic biomass," *Bioresource Technology*, vol. 199, pp. 42–48, 2016.

[3] J. Y. Zhu, G. S. Wang, X. J. Pan, and R. Gleisner, "Specific surface to evaluate the efficiencies of milling and pretreatment of wood for enzymatic saccharification," *Chemical Engineering Science*, vol. 64, pp. 474–485, 2009.

[4] W. Zhu, J. Y. Zhu, R. Gleisner, and X. J. Pan, "On energy consumption for size-reduction and yields from subsequent enzymatic saccharification of pretreated lodgepole pine," *Bioresources Technology*, vol. 101, pp. 2782–2792, 2010.

[5] X. Zhao, L. Zhang, and D. Liu, "Biomass recalcitrance. Part I: the chemical compositions and physical structures affecting the enzymatic hydrolysis of lignocellulose," *Biofuels, Bioproducts and Biorefining*, vol. 6, pp. 465–482, 2012.

[6] J. Xu, J. J. Cheng, R. R. Sharma-Shivappa, and J. C. Burns, "Sodium hydroxide pretreatment of switchgrass for ethanol production," *Energy Fuels*, vol. 24, pp. 2113–2119, 2010.

[7] N. Mosier, C. Wyman, B. Dale, R. Elander, Y. Y. Lee, M. Holtzapple, and M. Ladisch, "Features of promising technologies for pretreatment of lignocellulosic biomass," *Bioresource Technology*, vol. 96, pp. 673–686, 2005.

[8] K. Belkacemi, G. Turcotte, D. Halleux, and P. Savoie, "Ethanol production from AFEX-treated forages and agricultural residues," *Applied Biochemistry and Biotechnology*, vol. 70–72, pp. 441–462, 1998.

[9] Y. Chen, R. R. Sharma-Shivappa, D. Keshwani, and C. Chen, "Potential of agricultural residues and hay for bioethanol production," *Applied Biochemistry and Biotechnology*, vol. 142, pp. 276–290, 2007.

[10] R. A. Silverstein, Y. Chen, R. R. Sharma-Shivappa, M. D. Boyette, and J. A. Osborne, "A comparison of chemical pretreatment methods for improving saccharification of cotton stalks," *Bioresource Technology*, vol. 98, pp. 3000–3011, 2007.

[11] M. S. R. S. Rocha, B. Pratto, R. S. Júnior, R. M. R. G. Almeida, and A. J. G. Cruz, "A kinetic model for hydrothermal pretreatment of sugarcane straw," *Bioresource Technology*, vol. 228, pp. 176–185, 2017.

[12] J. Liu, Z. Gong, G. Yang, L. Chen, L. Huang, Y. Zhou, and X. Luo, "Novel kinetic models of xylan dissolution and degradation during ethanol based auto-catalyzed organosolv pretreatment of bamboo," *Polyerms*, vol. 10, p. 1149, 2018.

[13] H. Choi and J. S. Kwon, "Multiscale modeling and control of Kappa number and porosity in a batch pulp digester," *AIChE Journal*, vol. 65, no. 6, p. e16589, 2019.

[14] ——, "Modeling and control of cell wall thickness in batch delignification," *Computers & Chemical Engineering*, vol. 128, pp. 512–523, 2019.

[15] P. A. Wisnewski and F. J. Doyle, "Control structure selection and model predictive control of the Weyerhaeuser digester problem," *Journal of Process Control*, vol. 8, no. 5–6, pp. 487–495, 1998.

[16] S. Bhartiya, P. Dufour, and F. J. Doyle, "Fundamental thermal-hydraulic pulp digester model with grade transition," *AIChE Journal*, vol. 49, no. 2, pp. 411–425, Feb. 2003.

[17] J. Y. Yoo, "Technical and economical assessment of thermo-mechanical extrusion pretreatment for cellulosic ethanol production," Ph.D. dissertation, Kanas State University, Manhattan, KS, 2011.

[18] P. A. Wisnewski, F. J. Doyle, and F. Kayihan, "Fundamental continuous pulp-digester model for simulation and control," *AIChE Journal*, vol. 43, no. 12, pp. 3175–3192, 1997.

[19] R. M. Rowell, R. Pettersen, and M. A. Tshabalala, *Handbook of wood chemistry and wood composites, second ed.* Boca Raton, Florida: CRC Press, 2012.

[20] U. Vainio, N. Maximova, and B. H. J. Laine, "Morphology of dry lignins and size and shape of dissolved Kraft lignin particles by X-ray scattering," *Langmuir*, vol. 20, no. 22, pp. 9736–9744, 2004.

[21] G. Bali, X. Meng, J. I. Deneff, Q. Sun, and A. J. Ragauskas, "The effect of alkaline pretreatment methods on cellulose structure and accessibility," *ChemSusChem*, vol. 8, pp. 275–279, 2015.

[22] V. Arantes and J. N. Saddler, "Cellulose accessibility limits the effectiveness of minimum cellulase loading on the efficient hydrolysis of pretreated lignocellulosic substrates," *Biotechnology for Biofuels*, vol. 4, p. 3, 2011.

[23] H. J. Galicia, Q. P. He, and J. Wang, "A reduced order soft sensor approach and its application to a continuous digester," *Journal of Process Control*, vol. 21, no. 4, pp. 489–500, 2011.